

Experimental Characteristics of Continuously Variable Resonant Frequency Crystal Systems*

FLOYD DUNN, FRANK J. FRY, AND WILLIAM J. FRY
University of Illinois, Urbana, Illinois

(Received November 7, 1955)

The experimentally determined characteristics of a continuously variable resonant frequency crystal transducer are presented for the system operating under radiating conditions. These characteristics are presented for a high-power variable resonant frequency transducer of large radiating area, which utilizes the second harmonic and operates over the 2:1 frequency range from 22 kc to 44 kc with no more than a 2:1 variation in the pressure amplitude at a fixed point on the axis of the beam. Curves of pressure amplitude, input conductance, band width, half-power beam width, and efficiency, all as a function of the resonant frequency, are shown. The measured characteristics are compared with calculations based on a one-dimensional theory.

I. INTRODUCTION

FIXED resonant frequency transducers have been extensively studied and many references to them are to be found in the literature.¹ These units presently enjoy wide application in systems such as high-power ultrasonic generators and underwater sound detecting equipment.

The desirability of having variable resonant frequency transducers available is quite evident. To cite one example, a large number of such transducer systems, each tuned to a slightly different resonant frequency, can be operated in close proximity without mutual interference. With the system described in this paper it is possible to vary the frequency over a 2:1 range at constant driving voltage with a variation in the sound pressure amplitude of less than a factor of two.

Previous work with variable resonant frequency crystal systems is to be found in five papers by Fox and Rock,² Fry, Fry, and Hall,³ Hall and Fry,⁴ Welkowitz and Fry,⁵ and Fry, Dunn, and Fry.⁶ Fox and Rock presented experimental data on systems under non-radiating conditions utilizing quartz plates coupled to liquid columns. Fry, Fry, and Hall carried out a theoretical investigation of the various loss factors and the effect of different geometrical arrangements of the backing material and compared the theory with experimental results on laboratory models. Hall and Fry discussed certain design considerations of low loss variable resonant frequency crystal transducers. Welkowitz and Fry carried out detailed calculations based on the usual one-dimensional theory of piezoelectric

crystal systems for several particular variable resonant frequency crystal systems radiating into water. Fry, Dunn, and Fry presented detailed design and construction criteria for a large ADP-mercury transducer.

In this paper we present the experimentally determined characteristics of continuously variable resonant frequency crystal systems capable of delivering a large amount of acoustic radiation when operating into a liquid medium. The characteristics under radiating conditions which are of prime interest are the operating frequency range, efficiency, band width, input impedance, and power output, all as a function of frequency. The measured characteristics are compared with calculations based on a one-dimensional theory.⁶

II. DESCRIPTION OF THE TRANSDUCER

The details of the design and construction of this transducer are completely discussed in a companion paper.⁶ In this design the piezoelectric crystals are cemented with a rigid adhesive to a thin sheet of silver-palladium alloy. The alloy is spot-welded to a steel matrix for support. The mercury column is amalgamated to the alloy directly behind each crystal unit of the array. A piston is used to continuously vary the length of the mercury column. This in turn varies the resonant frequency of the composite system. The mercury chamber, including the piston face, is everywhere lined with an acoustic decoupling material (balsa wood in this case). The unit thus assembled is housed in a steel container having a ρ c-rubber window. The region between the crystal units and the rubber diaphragm is filled with degassed castor oil.

Figure 1 shows a photograph of the ADP crystal array of the transducer coupled to the mercury column. A portion of the gear mechanism for varying the length of the mercury column from a remote position and the mercury expansion chamber can also be seen. The unit is shown mounted on a dolly previous to being placed in the transducer housing. The crystal units are 45° Z-cut ADP and all have an over-all cross section 1 in. by 1 in. and are 2 in. long. The transducer radiating area is 12 in. by 12 in. The area of the mercury backing

* This research was supported by the U. S. Navy Bureau of Ships under Contract Nobsr 52367.

¹ For example, see the bibliographies in W. G. Cady, *Piezoelectricity* (McGraw-Hill Book Company, Inc., New York, 1946), and L. Bergmann, *Ultrasonics* (John Wiley and Sons, Inc., New York, 1946).

² F. E. Fox and G. D. Rock, *Proc. Inst. Radio Engrs.* **30**, 29 (1942).

³ Fry, Fry, and Hall, *J. Acoust. Soc. Am.* **23**, 94 (1951).

⁴ W. Hall and W. J. Fry, *Rev. Sci. Instr.* **22**, 155 (1951).

⁵ W. Welkowitz and W. J. Fry, *J. Acoust. Soc. Am.* **26**, 159 (1954).

⁶ Fry, Dunn, and Fry, *J. Acoust. Soc. Am.* **27**, 570 (1955).

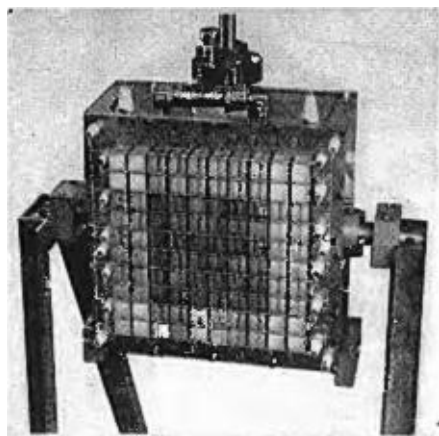


FIG. 1. Transducer motor shown mounted on the mercury housing.

chamber is 13 in. by 13 in. The 100 crystal units are composed of 16 1-ply units, 48 2-ply units, and 36 4-ply units and are arranged in parallel and tightly coupled to the mercury column of variable length. The choice of the above crystal units was determined by beam pattern considerations based on the Schelkunoff method of antenna analysis.⁷ The 36 4-ply units form the center portion of the array. Four 1-ply units make up each of the four corners and the remainder of the four sides of the array are each composed of 12 2-ply units.

III. EXPERIMENTAL METHOD

In making the experimental measurements we are primarily interested in locating the resonant frequency of the system and measuring the pressure amplitude of the acoustic disturbance produced in the liquid medium as a function of frequency. This can be done by using a piezoelectric crystal unit, operated far off resonance, as a pickup probe. The voltage generated by the crystal probe, as a result of the acoustic disturbance in its vicinity, is proportional to the amplitude of the acoustic pressure and can be measured by such laboratory instruments as an oscilloscope or a vacuum tube voltmeter. The resonant frequency of the transducer is

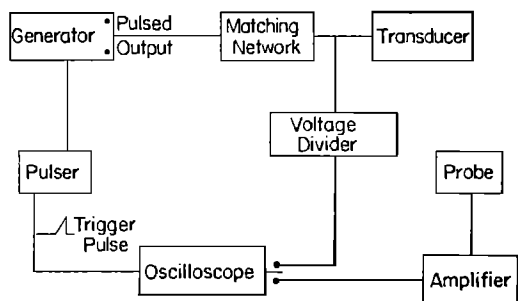


FIG. 2. Block diagram of the electronic driver and detector system.

defined as that frequency for which the greatest acoustic pressure is developed on the axis of the main beam as a function of frequency. The data thus obtained can be readily used for calculating such quantities as efficiency and band width.

In order to make accurate measurements of the acoustic pressure developed at the pickup probe by the direct transmitted beam, it is necessary that reflections from nearby objects not interfere with the signal traveling directly from the transducer to the probe. Such interferences serve to alter the acoustic pressure at the pickup probe and make it impossible to determine the magnitude of the transmitted signal. For this reason, a pulse method was found to be most suitable for the experiments described in this paper. The transducer is driven with a pulsed signal of such length that the trailing edge of the direct signal to the probe reaches the probe considerably sooner than the leading edge of the nearest reflection.

Figure 2 shows a block diagram of the electronic driver and detector system. The oscillator stage of the electronic generator is keyed on and off by an electronic pulser at the rate of approximately five pulses per

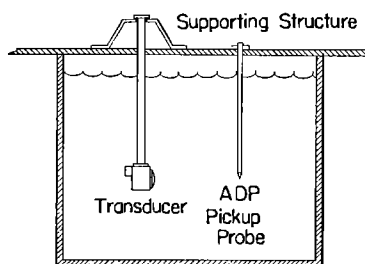


FIG. 3. Schematic diagram of the experimental arrangement.

second. The pulse length is approximately 600 μ sec. The pulse is simultaneously applied to the oscilloscope (which is used to measure both the transducer driving voltage and the probe voltage) to trigger the sweep circuit. The pulsed generator output voltage is applied to the transducer via a matching network, and a constant fraction of this voltage is presented to the oscilloscope for measurement. The probe voltage is amplified and presented to the oscilloscope for measurement. With the amplifier and oscilloscope used, the minimum detectable voltage developed by the probe is 100 μ v peak-to-peak. This corresponds to a pressure amplitude of 6.5 dynes/cm².

The experimental arrangement is shown schematically in Fig. 3. The tank is a wooden railroad water storage container approximately 11 ft high and 14 ft in diameter. The probe is a calibrated ADP hydrophone. Both the transducer and the probe can be rotated about 360° as well as be moved vertically and horizontally for positioning.

In obtaining the data for a variable resonant frequency crystal transducer the following procedure is followed: The mercury column of the transducer is set at a predetermined length. A frequency interval which

⁷ W. Welkowitz, *J. Acoust. Soc. Am.* **25**, 336 (1953).

includes the transducer resonant frequency for the chosen mercury column length is determined by calculations based on a one-dimensional theory. The frequency of the generator is then varied through this frequency interval and the probe voltage is recorded for constant driving voltage across the transducer. The frequency at which the probe voltage is a maximum is defined as the resonant frequency of the transducer. Curves of this type for the fundamental and second harmonic are shown in Fig. 4 where the parameter from curve to curve is the mercury column length.

IV. RADIATING CHARACTERISTICS

Figure 4 shows representative curves of the relative pressure amplitude of the fundamental and second harmonic developed at the probe as a function of frequency. The numbers adjacent to the curves indicate the length of the mercury backing column for which

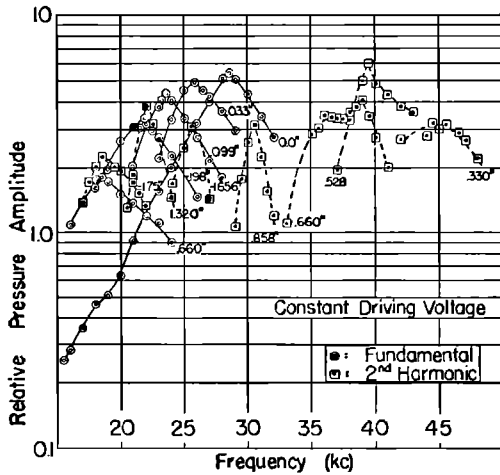


FIG. 4. Relative pressure amplitude versus frequency for the fundamental and second harmonic of the transducer under constant driving voltage. The parameter from curve to curve is the mercury backing length.

the data were obtained. The curve for zero mercury backing length for the fundamental is shown extending below the resonant frequency from 28.5 kc to 15.5 kc. The desirability of operating the variable frequency transducer at resonance can be readily seen when the relative pressure amplitudes from this curve are compared with those of the other curves at resonance. For example, the ratio of the relative pressure amplitudes at 23.5 kc for the curve with 0.099 in. of mercury backing and the zero mercury backing curve is 2.35, or a power ratio of 5.5. If we consider the ratios at 18.5 kc for the curve with 0.660 in. of mercury backing and the zero mercury backing curve, the relative pressure amplitude ratio is 3.6 and the power ratio is 12.96. In other words, thirteen times the power can be radiated into the water medium for the same driving voltage for a frequency shift of 35% by operating the transducer at its resonant frequency. This offers a great advantage

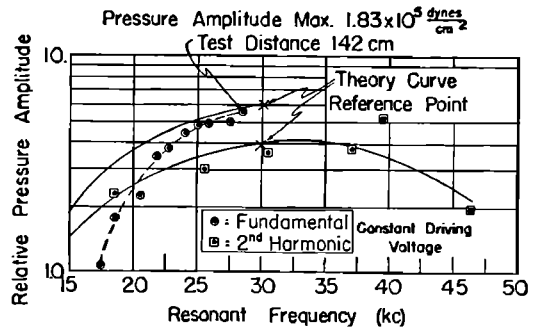


FIG. 5. Relative pressure amplitude versus resonant frequency for the fundamental and second harmonic.

when relatively high power is desired, and the voltage breakdown of the piezoelectric crystal unit must be considered.

Figure 5 shows the relative pressure amplitude at the resonant peaks for the fundamental and second harmonic as a function of resonant frequency. The fundamental is shown shifted from 28.5 kc to 17.5 kc, a frequency shift of 34.6%. The second harmonic is shown in the frequency interval 46.5 kc to 18.5 kc, a frequency shift interval of 22.5% to 69.1%. Within the frequency interval of 22 kc to 44 kc, a 2:1 frequency interval, it is seen that the relative pressure amplitude operating on the second harmonic, for constant driving voltage, does not vary by more than a factor of two. Comparing this with the variation of the relative pressure amplitude of the fundamental from 17.5 kc to 28.5 kc it is seen that the second harmonic is more suitable for operating over a 2:1 frequency range. The theoretical curves were obtained from calculations based on a one-dimensional theory.⁵ These curves show the theoretical variation of the relative pressure amplitude as a function of the resonant frequency and include corrections for beam spreading effects. The relative pressure amplitudes of the "reference points" are arbitrarily chosen so that comparisons could be

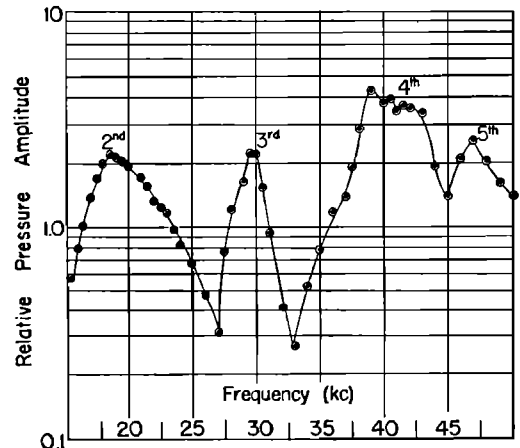


FIG. 6. Relative pressure amplitude versus resonant frequency with 1.75 in. of mercury backing.

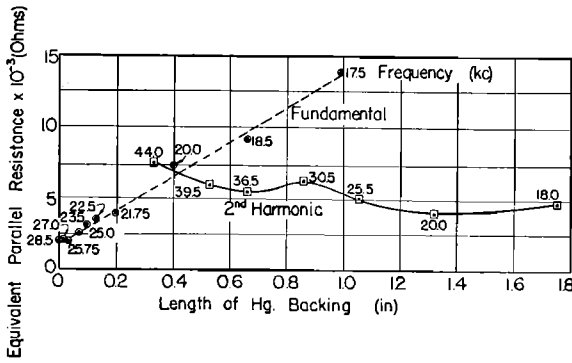


FIG. 7. Equivalent parallel resistance *versus* length of mercury backing for the fundamental and second harmonic.

made with the measured values and their frequencies were chosen as 30 kc—the fundamental resonant frequency of the transducer motor before being coupled to the mercury column. Concerning the second harmonic, it is seen that the variation of the relative pressure amplitude with the resonant frequency is in rather good agreement in the frequency range from 18.5 kc to 46.5 kc. The desirability of operating the transducer at the second harmonic in preference to the fundamental is most evident from this curve, for it is seen that for minimum variation in the transducer power output, the second harmonic makes twice the frequency range available.

Figure 6 shows the relative pressure amplitude as a function of frequency for 1.75 in. of mercury backing. The resonance curves of the second through the fifth harmonics are shown from 15.5 kc to 50 kc, the frequency range of the electronic driver. For this length of mercury backing, all the harmonics have been shifted to approximately 31% of their zero shift frequency. The fundamental frequency for this quantity of mercury backing would appear at approximately 12 kc. This curve shows that the harmonics are sufficiently separated in frequency, so that there should be no

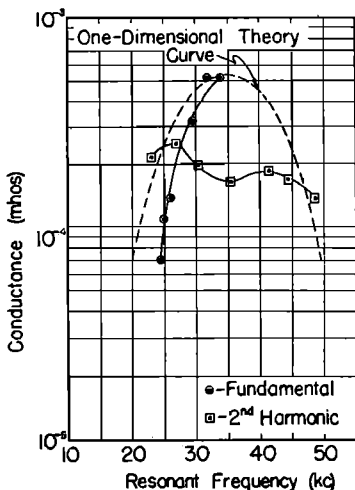


FIG. 8. Conductance *versus* resonant frequency for the fundamental and second harmonic.

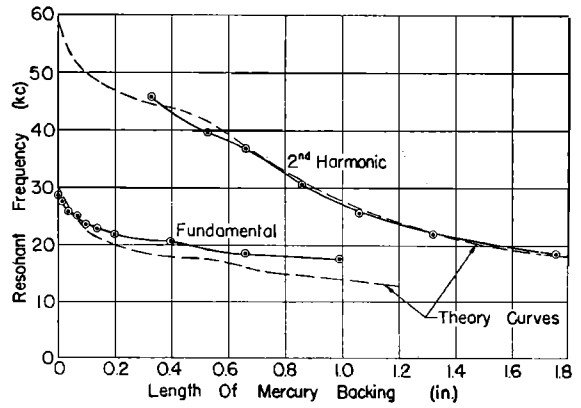


FIG. 9. Resonant frequency *versus* length of mercury backing for the fundamental and second harmonic.

danger of confusing them in the event that it is desirable to operate the transducer at a higher harmonic. The curve also shows that the relative amplitudes of these harmonics vary by only a factor of two.

The input impedance of the transducer was measured at resonance at a number of frequencies for the fundamental and second harmonic. The equivalent parallel resistance of the input impedance of the transducer is shown in Fig. 7 plotted as a function of the length of mercury backing. It is interesting to note that the resistance of the second harmonic is not predicted by the one-dimensional theory.⁵ The theoretical variation of the conductance of the transducer at resonance as a function of the resonant frequency is shown in Fig. 8 together with the experimentally determined values for the fundamental and second-harmonic frequencies of the transducer. The zero shift frequency of the transducer was taken the same as that of Fig. 5 (the reference point). It is seen that the fundamental agrees rather well with the one-dimensional theory—the slope of the experimentally determined conductance

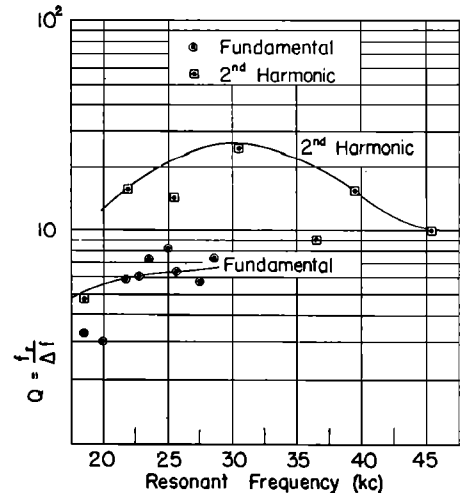


FIG. 10. Q *versus* resonant frequency for the fundamental and second harmonic.

curve being slightly greater than that predicted. However, the slope of the experimentally determined second harmonic conductance curve does not even approximate the theoretical curve.

Figure 9 shows the variation of the resonant frequency as a function of the length of mercury backing for the fundamental and second-harmonic frequencies. The one-dimensional theoretical curves⁶ are also shown. Here it is seen that the second harmonic is in comparatively better agreement with the theory than is the fundamental.

The Q 's ($f_r/\Delta f$), for the fundamental and the second harmonic were computed from the curves of Fig. 4. These are shown as a function of the resonant frequency in Fig. 10. Curves from the one-dimensional theory⁶ are also shown. The data for the fundamental frequencies are considerably scattered about the theoretical

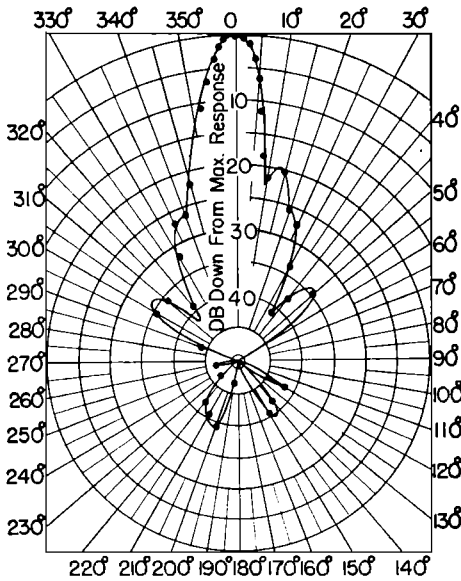


FIG. 11. Normalized transmitting response of the second harmonic at 20.75 kc, 0.858 in. of mercury backing.

curve while those of the second harmonic appear to agree rather well with the theory. As the theory indicates, the order of magnitude of the Q 's in the frequency range from 20 kc to 30 kc is 5 to 7 for the fundamental and that of the second harmonic is 10 to 25 in the frequency range from 22 kc to 45 kc. The theory also indicates that harmonics higher than the second should have even higher Q 's. For example, the theory suggests that a Q of 50 could be obtained if the third harmonic were utilized.

Figures 11 and 12 show typical normalized radiation patterns of the second harmonic of the transducer operating at resonance in the frequency range from 20.75 kc and 0.858 in. of mercury backing to 35.0 kc and 0.66 in. of mercury backing. The test distance was 142 cm. The variation of the half-power beam width as a function of the resonant frequency for the fundamental

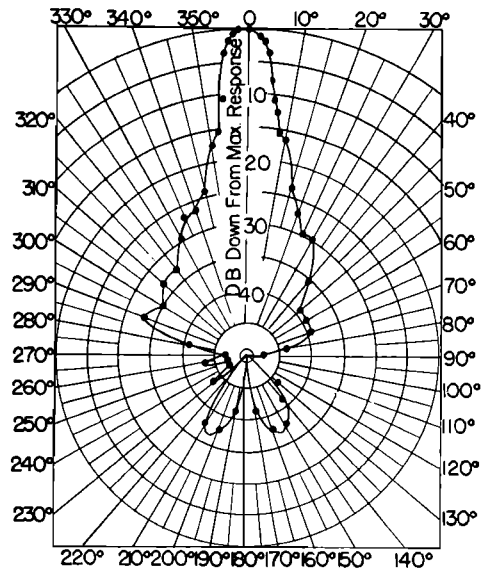


FIG. 12. Normalized transmitting response of the second harmonic at 35.0 kc, 0.66 in. of mercury backing.

and second harmonic is shown in Fig. 13. It is seen that the fundamental beam widths varies from 12.5° to 9° in the frequency range from 18.5 kc to 28.5 kc and the second-harmonic beam width varies from 12.5° to 6° in the frequency range from 22 kc to 45 kc. The beam pattern curves show that in both cases the minor lobes are suppressed 18 db or more below the peak of the main lobe. This was the case throughout the region of investigation.

The power input to the transducer was determined, at the resonant frequencies for which beam patterns were taken, from the measured values of the electrical input impedance and the transducer driving voltage. The power output was obtained by integrating the beam pattern. While this does not give results of great accuracy, it offers an approximate calculation of the efficiency. The efficiency of the transducer (defined as $P_{out}/P_{in} \times 100$) as a function of the resonant frequency is shown in Fig. 14 for the fundamental and the second

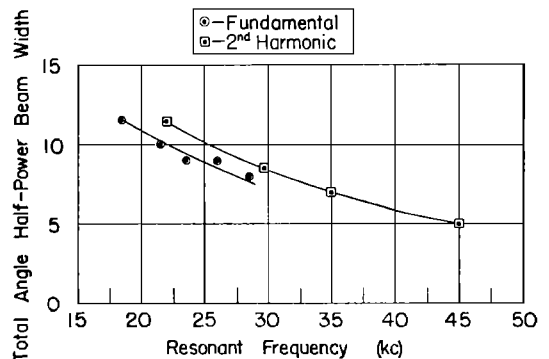


FIG. 13. Total angle half-power beam width versus resonant frequency for the fundamental and second harmonic.

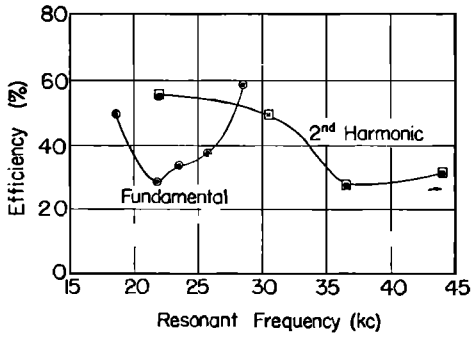


FIG. 14. Efficiency *versus* resonant frequency for the fundamental and second harmonic.

harmonic. It is seen that the efficiency of the fundamental decreases from approximately 57% at 28.5 kc and zero mercury backing to 30% at 21.75 kc and 0.198 in. of mercury backing and then increases to 48% at 18.5 kc and 0.66 in. of mercury backing. On the other

hand, the efficiency of the second harmonic increases from 20% at 45 kc and 0.33 in. of mercury backing to 55% at 22 kc and 1.32 in. of mercury backing.

V. SUMMARY

High-power continuously variable resonant frequency crystal transducers of large radiating area can be built and operated successfully over a 2:1 frequency range by utilizing the second harmonic. The maximum variation of the power output of such a transducer in the 2:1 frequency range is less than a factor of four. For the ADP-mercury system described in this paper, the efficiency of the transducer operating on the second harmonic increases with the addition of the mercury backing in the frequency range from 45 kc to 22 kc.

VI. ACKNOWLEDGMENTS

The authors wish to thank Mr. Leroy Dryer for contributions to this investigation.